Comparison of material sources and customer locations for commercial space resource utilization

Merel VERGAAIJ[a,*], Colin R. McINNES[a], Matteo CERIOTTI[a]

[a] *James Watt School of Engineering, University of Glasgow, G12 8QQ, Glasgow, United Kingdom*

Abstract

Space resource utilization (SRU) can be a catalyst for a growing space economy. Significant reductions in cost, launch mass and risk for human and robotic activities beyond Earth can be achieved. Commercial entities will have the opportunity to generate revenue through economic development, allowing for a decreased dependency on governmental agencies for the exploration of space. A wide variety of materials can be found on planetary and small solar system bodies, which are potentially of great use to customers in space. This paper conducts a comparison of the economic and commercial potential of SRU on the surface of the Moon, Mars, a representative near-Earth asteroid and a representative main-belt asteroid. In particular, mining of water will be considered which will be electrolyzed into hydrogen and oxygen using solar power. Coupled economic and trajectory optimization then results in the minimum specific cost to deliver propellant (LOX/LH_2) from these bodies to a number of customer locations. Customers on the surface of or in orbit around the Earth, Moon, and Mars are investigated, along with Psyche, a large metallic main-belt asteroid. Using a cost model that considers technology maturation to allow current aviation-like costs to be used for development and manufacturing, missions are optimized. Results show that for customers beyond low-Earth orbit, SRU should be used instead of launching water-derived resource directly from the Earth. In particular, near-Earth asteroids are shown to be in an attractive location for mining, processing and delivering a large quantity of LOX/LH_2 at a low specific cost, for customers in the vicinity of the Earth and the Moon, including nearby collinear Lagrange points. Exceptions are customers on the surface of the Earth and the Moon, who, together with customers on the surface of Mars, are better off mining and processing on that same surface. A sensitivity analysis shows that, for all investigated customers except Psyche, there are near-Earth asteroids available which can be used to deliver water-derived resources for a lower specific cost than the most ideal main-belt asteroid. Only once these near-Earth asteroids have been depleted, mining main-belt asteroids and transporting resources back to a customer in the vicinity of the Earth is worth considering.

Keywords: Space resource utilization, economic modelling, trajectory optimization, Lunar mining, Martian mining, asteroid mining

1. Introduction

The cost, mass and risk of human and robotic activities beyond Earth can be significantly reduced through space resource utilization (SRU) [1]. SRU is the strategy of using natural resources from the Moon, Mars and other bodies for use in situ or elsewhere in the solar system, which can replace material that would otherwise be brought from Earth [2]. There are clearly many advantages to SRU. By not having to transport propellant for both the outbound and return segments of a mission, the total mass that has to be lifted from Earth's deep gravity well can be reduced, or the payload capability can be increased. Risk can be reduced by providing a back-up and in-situ capability for human life support so mission capabilities and flexibility can be increased [3]. The use of SRU may also provide a means for commercial entities to earn revenue through space exploration by delivering resources

*Corresponding author, merel.vergaaij@glasgow.ac.uk

[4–7], such as propellant electrolytically split from water, to a range of customers at different locations in the inner solar system.

Opportunities for SRU have been researched for decades, focused on the Moon [8–12], Mars [3, 8, 11, 13] and asteroids [14–16]. Potential materials to utilize include O_2 and H_2O for life support, LOX and LH_2 for propellant and various metals, and elements and compounds for metallurgic and chemical production processes [12]. Where space exploration missions were driven solely by government agencies, this is now being complemented by commercial enterprises. SRU can be the catalyst for a growing space economy [17], with enterprises processing resources and delivering products to customers at a range of locations.

Because of the interest of commercial companies, a range of economic assessments has been published in recent years, investigating the use of SRU on various planetary bodies [15, 17–20]. These works address specific mission architectures with an impressive level of detail, as well as an array of economic models. Where appropriate selection of cost models, methods and tools is already a difficult task for space engineering [21], in addition, there are many different assumptions involved in the separate economic assessments, as well as different decisions for mission architectures. Comparison of different economic assessments is therefore complicated.

This work aims to explore the economic and commercial potential of SRU at a number locations for customers in various locations, through a parametric approach. Using the same economic model, applied to a range of different mission architectures, allows for an unbiased comparison. Because of the many parameters involved in the economic model and mission analysis, a balance in the level of approximation used is essential. This results in a moderately low-fidelity parametric approach that can be applied to many different combinations of resource and customer locations. This parametric approach is based on an economic model coupled with trajectory optimization, used to compute the specific cost for delivering propellant (LH_2 and LOX) as a product to customers. The results can be used to identify potential value chains to focus further research using high-fidelity models.

The structure of this paper is as follows. First, Section 2 elaborates on the methodology for this work, starting with the adopted baseline mission architecture, economic modelling and trajectory optimization. Following this, Section 3 presents and discusses the obtained baseline results. This is followed by a sensitivity analysis in Section 4 and the paper is concluded in Section 5.

2. Methodology

The goal of this paper is to identify combinations of material sources and customer locations for which mining, processing and selling LOX/LH_2 can be profitable. Missions starting at the Earth, mining at the source, and delivering the resources to various customer locations will be investigated. The following sources are proposed:

1. Earth surface
2. Lunar surface
3. Representative near-Earth asteroid (NEA)
4. Martian surface
5. Representative main-belt asteroid (MBA)

More specifically, the NEA 2000 SG344 [22, 23] and the MBA 2015 AE282 are considered, based on favorable orbital characteristics (i.e., close proximity to the Earth's orbit and in the inner belt, respectively, as well as a low inclination) and brightness (which relates to its size). However, in Section 4.3 a search of other asteroids is conducted to assess the importance of specific target asteroid selection. It is assumed that these asteroids are water-bearing C-type asteroids.

Customer locations to be considered are:

1. Earth surface
2. Low-Earth orbit (LEO), 400 km, similar to the International Space Station
3. Geostationary orbit (GEO)
4. Sun-Earth L_1-point (SE-L_1)
5. Sun-Earth L_2-point (SE-L_2)
6. Lunar surface
7. Low Lunar orbit (LLO), 100 km circular orbit
8. Lunar Gateway
9. Martian surface
10. Mars Base Camp, elliptical orbit, 1 sol period, 400 km periapsis [24]
11. Sun-Mars L_1-point (SM-L_1)
12. 16 Psyche, a metallic MBA

These destinations are considered because of the need for water and other volatiles, either for human consumption or as propellant [25]. The Lunar Gateway is a proposed modular space station located in a stable orbit around an Earth-Moon Lagrange point, which will be used to test and verify

technologies and procedures for crewed missions in deep space [26]. The Mars Base Camp is a proposed space station to be assembled in orbit around Mars [24]. Psyche is considered as a possible destination since it is a large metallic M-type asteroid and in order to mine metals, water is required [27]. All possible combinations are investigated, leading to 60 scenarios that have to be optimized. A schematic showing the wide spread of source and customer locations is presented in Figure 1 with labels corresponding to the two lists above.

This section now sets out the various aspects of the analysis to be undertaken, starting with the mission architecture that will be investigated. Next, the methodology used for economic modelling is explained, followed by the mass budget calculations used in this economic model. This is followed by the methodology used to find trajectories between the Earth, the material source and customer locations. Finally, the optimization method used in this work is set out.

2.1. Mission architecture

A baseline mission architecture is presented in Fig. 2. A single consistent architecture is considered for all scenarios to allow comparisons, because the objective is to produce data to allow a top-level comparison and evaluation of material sources and customer locations. Based on the specific scenario, i.e. a given combination of material source and customer location, this architecture can be adapted. Details for these adapted mission architectures will be presented below, after the definition for the baseline mission architecture.

The baseline scenario starts with a launch to LEO using SpaceX's Super Heavy and Starship, for which a circular orbit with an altitude of 185 km is assumed based on previous SpaceX launches [28]. The maximum payload capacity of the launch vehicle (estimated at 150 tons, i.e. 136 metric tonnes [28]) is used to size a cargo spacecraft, the mining and processing equipment (MPE) required and the propellant needed for the first orbit transfer manoeuvre. Subsequently, the cargo spacecraft, loaded with the MPE, departs from LEO to transfer to the material source. After arrival at the material source location, the MPE is installed and mining and processing water into propellant can start, producing LOX and LH_2. When the mining phase has completed, the cargo spacecraft transfers to the location of the resource customer. During this transfer, the cargo spacecraft utilizes part of the mined and processed payload as propellant. At the destination, the remaining propellant will be sold to the customer.

The specific mission architecture is dependent on the combination of material source and customer location. Exceptions and clarifications to the above mission architecture are as follows:

- Missions with the material source on the Earth's surface do not include MPE, because the volatiles are already available in processed form and so are delivered directly to the customer.
- Missions landing on the Earth or Martian surface are equipped with an entry, descent and landing system (EDL) to cope with atmospheric (re-)entry. (Re-)entry is performed using a direct descent from a hyperbolic capture orbit.
- In absence of an atmosphere on the Moon, the cargo spacecraft is assumed to be soft-landed on the Lunar surface, from an intermediate low-Lunar orbit.
- For interplanetary transfers and transfers to Lagrange points, time-dependent Lambert arcs are employed. Transfers to escape and from capture are modelled as hyperbolic trajectories.
- Spacecraft launching from the Lunar or Martian surface transfer through an intermediate circular orbit (at 100 km) before escape and further transfer to their destination.

2.2. Economic model

For each mission scenario, the minimum specific cost to acquire resources and deliver them to a customer location is calculated (in $ per kg of delivered resources). In order to do so, the total cost for the mission has to be calculated, which is done similarly to Refs. [22, 23]. A summary is presented here, but the reader is referred to these papers for further details. Cost contributions that are included are for launch (C_l), development (C_{dev}), manufacturing (C_{man}), operations (C_{op}) and propellant (C_{prop}). It is assumed that the missions take place in a mid- to far-term time frame, which is reflected in the costs, i.e. it is assumed that technology has matured through intermediate missions and development and manufacturing costs are represented by

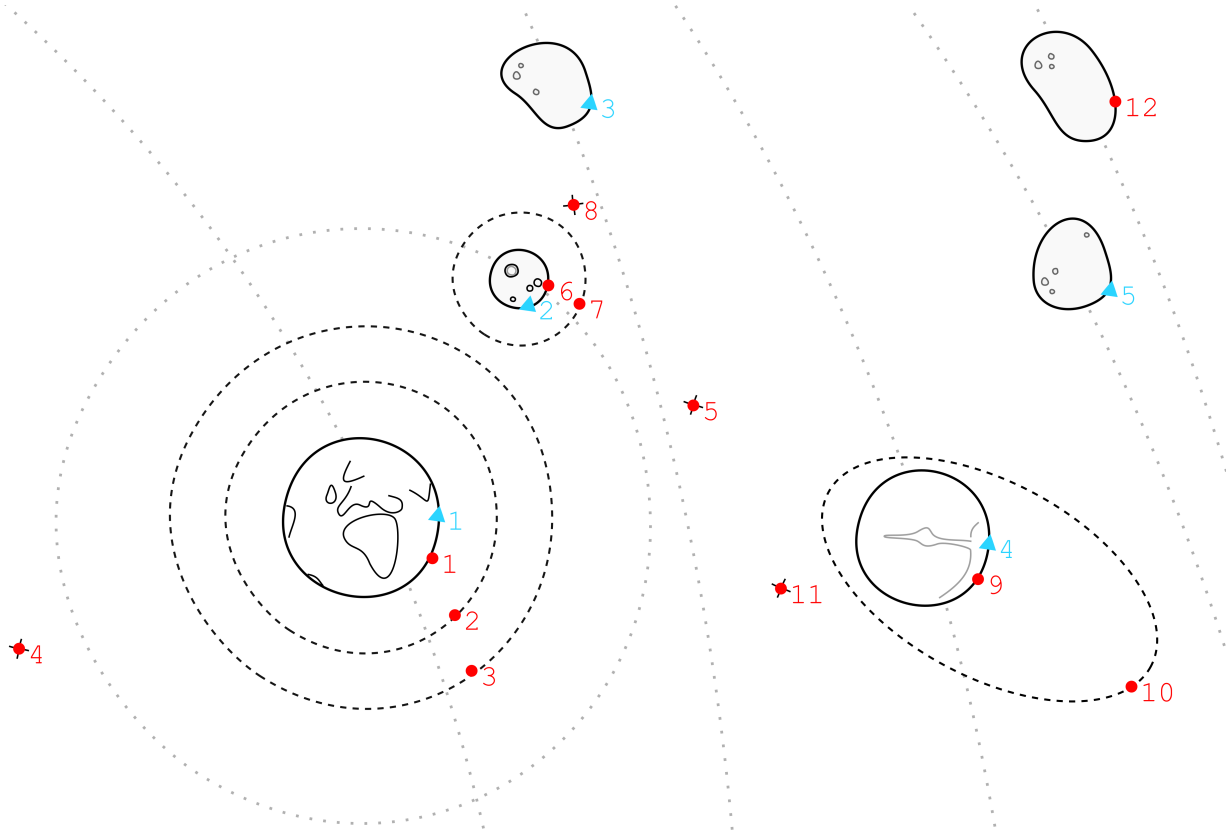

Figure 1: Schematic showing the source and customer locations. Source locations labelled with blue triangles: 1) Earth surface, 2) Lunar surface, 3) NEA, 4) Martian surface, and 5) MBA. Customer locations labelled with red circles: 1) Earth surface, 2) LEO, 3) GEO, 4) SE-L_1, 5) SE-L_2, 6) Lunar surface, 7) LLO, 8) Lunar Gateway, 9) Martian surface, 10) Mars Base Camp, 11) SM-L_1, and 12) Psyche.

aviation-like costs. All results in this paper assume that there will be a time-frame where this assumption holds. Values for these cost elements are given in Table 1 and further explanation is given below.

Table 1: Cost elements used for modelling.

Cost element	**Value [FY2020$]**	
C_l	13.10×10^6	
C_{dev}	37.19	/kg
C_{man}	1007.1	/kg
C_{op}	6.98×10^6	/year
C_{prop}	0.95	/kg

To compute the total cost, C, specific costs for the elements are multiplied by the total mass or time for that element:

$$C = C_l + (C_{dev} + C_{man})m_{dry} + C_{op}t_{mis} + C_{prop}m^O_{prop} \quad (1)$$

in which m_{dry} is the combined dry mass of the cargo spacecraft and MPE (in kg), t_{mis} the mission duration (in years) and m^O_{prop} the propellant required for the outbound transfer with the cargo spacecraft (in kg). The next section will elaborate on the calculation of these elements.

Finally, the specific cost, c (in $/kg), can be calculated using:

$$c = \frac{C}{m_{r,sold}} \quad (2)$$

in which $m_{r,sold}$ is the resource mass sold at the customer location (in kg).

2.3. Mass budget calculations

This section describes the method for calculating the mass budget of the proposed missions, based on the method proposed in earlier work in Ref. [23]. As described in Section 2.1, all missions start with a Starship system (Super Heavy

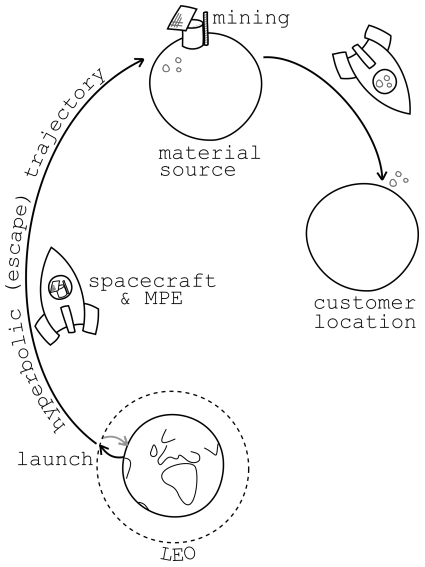

Figure 2: Baseline mission architecture.

and Starship combined) utilized at maximum payload capacity. This payload capacity (m_l) is divided over the dry mass for the cargo spacecraft loaded with the MPE ($m_{s/c,dry}$) and the propellant for the initial transfer manoeuvre (m^O_{prop}):

$$m_l = m_{s/c,dry} + m^O_{prop} \tag{3}$$

First, the propellant requirement m^O_{prop} is calculated:

$$m^O_{prop} = m_l \left(1 - e^{-\frac{\Delta V^O}{I_{sp} g_0}}\right) \tag{4}$$

in which ΔV^O is the velocity change required to transfer from the LEO parking orbit to the material source location and I_{sp} is the specific impulse of the propulsion system. Section 2.4 will detail how ΔV^O is obtained for the separate missions. The propulsion system used throughout this work is assumed to be LOX/LH_2 with $I_{sp} = 446$ s, to allow the use of in-situ propellant manufactured from water. The total dry mass of the cargo spacecraft loaded with MPE can then be calculated from Eq. (3).

Next, the total dry mass of the composite spacecraft, $m_{s/c,dry}$, is split using a mass fraction, λ_{MPE}, which will be optimized later:

$$m_{s/c,dry} = m_{cargo} + m_{MPE} \tag{5a}$$
$$m_{MPE} = m_{s/c,dry}\lambda_{MPE} \tag{5b}$$
$$m_{cargo} = m_{s/c,dry}(1 - \lambda_{MPE}) \tag{5c}$$

The total quantity of volatiles that is mined and processed at the source, $m_{r,mined}$ is determined by: m_{MPE}, the duration of the mining phase (t_{mining} in days), and the throughput rate (r in kg/day/kg of MPE), such that

$$m_{r,mined} = m_{MPE} r t_{mining} \tag{6}$$

in which t_{mining} is related to the stay time at the asteroid, Δt_{stay}, by:

$$t_{mining} = \Delta t_{stay} - 14 \text{ days} \tag{7}$$

to account for proximity operations, installing the MPE and transport of the resources to the cargo spacecraft.

The throughput rate to mine water and process it into LOX/LH_2 is calculated similar to the method described in Ref. [23], using values from Refs. [29–31], but incorporates a different water content of the regolith at the various material sources, as well as a different solar distance. Mass is included for the structure, equipment for collecting, grinding, separating gases from solids, condensing vapors, electrolysis, solar panels to supply power for the mining and electrolysis equipment, as well as a 10% margin for uncertainty. Where Ref. [23] finds a throughput rate for NEAs (at a distance of 1 AU) of 1.47 kg/day per kg of MPE, this work includes correction factors for:

- *Water content*, which affects the amount of water extracted from the same quantity of regolith. The same mass of equipment is required to process the same amount of regolith, but this results in less harvested water. A water content of 10% is assumed for water-bearing asteroids [30], but only 1.3% for typical Martian regolith [8, 13] and 1.5% for typical Lunar regolith [8].
- *Solar distance*, which influences the solar flux and therefore the performance of the solar panels to power the mining and processing equipment. This change in performance has an effect on the total solar panel mass required to power the equipment for mining, processing and electrolysis. The throughput in Ref. [23] has been calculated at a solar distance of 1 AU, and an approximation for the solar panel performance is based on an inverse-quadratic relationship with the semi-major axis (in AU) of the material source body.

This results in throughput rates for the separate material sources as shown in Table 2.

Table 2: Assumed throughput rate for all sources.

Source	**r [kg/day/kg of MPE]**
Earth surface	N/A
Lunar surface	1.358
NEA 2000 SG344	1.538
Martian surface	0.602
MBA 2015 AE282	0.365

One issue not taken into account in Ref. [23] is the combustion mixture ratio of LOX/LH_2, since the MPE produces LOX/LH_2 in a stoichiometric ratio (i.e. the ratio at which complete combustion takes place, which is the resulting ratio after electrolysis, $\sim 7.9:1$). However, current propulsion systems are designed for a fuel-rich mixture ratio, meaning that there is an excess of oxygen after electrolysis. A mixture ratio of $6.5:1$ is adopted in this work, which is slightly higher than currently used $(6:1)$, but still considered very reasonable [32]. The closer the mixture ratio is to the stoichiometric ratio, the smaller the excess of oxygen. In this model, the excess oxygen is vented, which is a common approach [8, 25, 32]:

$$m'_{r,mined} = m_{r,mined}\lambda_{MR} \tag{8}$$

in which $m'_{r,mined}$ is the total quantity of volatiles after venting the excess oxygen, and λ_{MR} the fraction that has to be vented in order to reach a combustion mixture ratio of $6.5:1$.

The quantity of resources that can be transported to the customer location is then calculated using:

$$m_{r,transportable} = \frac{1-\epsilon_{min}}{\epsilon_{min}} m_{cargo} \tag{9}$$

in which the minimum allowed structural coefficient is $\epsilon_{min} = 0.1$ [33] for all spacecraft considered in this work. Equation (9) means that the total resource mass, m_r is determined by: $m_r = \texttt{max}\left\{m'_{r,mined}, m_{r,transportable}\right\}$. For the NEA and MBA, an additional check is performed to ensure that the asteroid is sufficiently large to supply m_r, consistent with Ref. [23].

Finally, because the cargo spacecraft employs in-situ resource utilization, consuming part of the LOX/LH_2, the quantity of resources that can be sold at the customer destination is equal to:

$$m_{r,sold} = m_r - m^I_{prop} \tag{10}$$

in which m^I_{prop} is the required propellant mass for the inbound transfer, i.e. the transfer to the customer location. The quantity of propellant required is calculated using:

$$m^I_{prop} = (m_{cargo} + m_r)\left(1 - e^{-\frac{\Delta V^I}{I_{sp} g_0}}\right) \tag{11}$$

where ΔV^I is the velocity change required to go from the source to the destination. Depending on the scenario, this can include a launch from a planetary or lunar surface. Section 2.4 will detail the method for determining this ΔV.

2.4. Trajectories

The missing parameters to calculate the specific cost are the ΔV requirements for the various transfers. This section explains how these are calculated for each scenario.

A patched-conic approach is used, connecting a number of relevant two-body systems. Ephemerides of planetary bodies and asteroids are taken from JPL databases [34, 35]. As noted in Section 2.1, interplanetary segments of the transfers are modelled using Lambert arcs, while transfers between closed orbits around the Earth or Mars are modelled using Hohmann transfers. Transfers to escape or from capture are modelled using hyperbolic trajectories with an impulse approximation. The methodology for calculating ΔV^O and ΔV^I and an example are given below.

The ΔV and transfer time, t_t, for each segment can be determined using one of four ways:

1. A two-burn Hohmann transfer, used to calculate ΔVs between two closed orbits around the Earth or Mars. Between circular and elliptical orbits around the same main body, ΔV and t_t are both calculated using the Hohmann transfer, taking the inclination change into account where necessary.
2. For transfers from a circular or elliptical orbit to escape, or from capture to a circular or elliptical orbit, a single ΔV is applied. The hyperbolic escape orbits are designed such that the excess velocity, v_∞, is equal to the ΔV of the next segment of the escape orbit, or the previous segment of the capture orbit. A single ΔV is applied at periapsis of the hyperbolic transfer orbit. The transfer time, t_t, is estimated as the time from periapsis of the transfer orbit to the sphere of influence of the main body.

3. A Lambert arc is used to calculate interplanetary transfers between bodies (e.g., Earth escape to Mars capture or NEA), as well as transfers to Lagrange points. Where applicable, the ΔV at the start (ΔV_1) and end (ΔV_2) of the Lambert arc is used to compute the hyperbolic trajectories. The timing, and thereby ΔV requirement of these Lambert arcs is optimized in Section 2.5. The Lambert solver used in this paper is coded in Python [36], but translated to MATLAB®, to be used in conjunction with the genetic algorithm explained in Section 2.5.
4. Fixed values of ΔV or t_t for certain segments, as listed in Table 3. For atmospheric (re)-entry, a ballistic trajectory followed by a direct descent is assumed. For transfers to and from the parking orbits at 100 km, the value for t_t is set to zero, because determining this parameter accurately is outside the scope of the paper and this duration is negligible compared to the duration of the other segments. Otherwise t_t is approximated by the time taken to transfer from the edge of the sphere of influence, along a parabolic capture trajectory with periapsis at the surface, to the periapsis of that trajectory. SpaceX states that over 99.9% or 99% of the energy is dissipated aerodynamically during Earth and Mars atmospheric entry [37], respectively, but supersonic retro-propulsion is necessary to land on Mars [38]. The estimated ΔV given for this propulsive descent is based on the Mars Design Reference Architecture 5.0 [39], which also utilizes supersonic retro-propulsion for the descent on Mars.

Table 3: Fixed segment ΔV and t_t.

Segment	**ΔV [km/s]**	**t_t [days]**
Earth capture → Earth surface	0 [39]	7.8
Mars capture → Mars surface	0.595 [39]	11.7
LLO (100 km) → Lunar surface	1.963 [40]	0
Lunar surface → LLO (100 km)	1.905 [40]	0
Mars surface → LMO (100 km)	4.028 [41]	0

An example is given below for the scenario where resources are mined on the Lunar surface and transported to the Mars Base Camp, which is in an elliptical orbit with a period of one Martian day (1 sol) and periapsis at 400 km [24]. Figure 3 illustrates where the separate impulsive ΔVs are applied. This example utilizes all four methods to determine ΔV and is one of the more complex calculations:

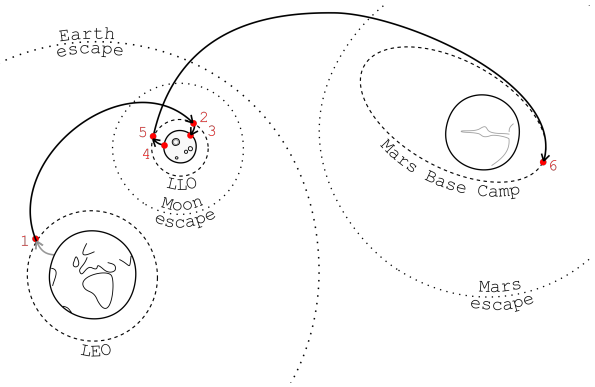

Figure 3: Schematic for example trajectory for scenario "Lunar Surface → Mars Base Camp". Red circles showing where the impulsive ΔVs are applied.

- Outbound, ΔV^O
  1. ΔV at periapsis of a Hohmann transfer orbit from a LEO parking orbit to Lunar capture;
  2. ΔV at periapsis of a hyperbolic trajectory to LLO (100 km), with v_∞ equal to the ΔV at apoapsis of the Hohmann transfer orbit from the LEO parking orbit to Lunar capture;
  3. Given ΔV for powered descent from LLO to lunar surface, from Table 3.
- Inbound, ΔV^I
  4. Given ΔV for powered ascent to LLO (100 km);
  5. ΔV at periapsis of a hyperbolic trajectory from LLO to lunar escape, with $v_\infty = v_p - v_{Moon}$, in which v_{Moon} is the circular velocity of the Moon around the Earth and v_p is the velocity at periapsis of a hyperbola from lunar escape to Earth escape with $v_\infty = \Delta V_1$ of an Earth-Mars Lambert arc;
  6. ΔV at periapsis of a hyperbola from Mars capture to Mars Base Camp with $v_\infty = \Delta V_2$ of the Earth-Mars Lambert arc.

In combination with the information given in Section 2.3, all variables to compute the total cost and specific cost for Eqs. 1 and 2 can now be determined.

2.5. Optimization

There are a number of parameters that have to be optimized for each scenario, in order to find the lowest specific cost, c, for each scenario.

A genetic algorithm is now employed to find a global optimum without the need for an initial guess [22, 23, 42, 43]. The built-in genetic algorithm in MATLAB® is used, using default parameter settings, except for the initial population, which is uniformly randomly spread throughout the whole domain. The general decision vector for the genetic algorithm is as follows:

$$\mathbf{X} = \begin{bmatrix} \Delta t^O & \Delta t_{stay} & \Delta t^I & t^I_{dep} & \lambda_{MPE} \end{bmatrix} \quad (12)$$

in which Δt^O is the transfer time for the outbound Lambert arc, Δt_{stay} the stay time at the asteroid, Δt^I the transfer time for the inbound Lambert arc, t^I_{dep} the departure date for the inbound transfer and λ_{MPE} the mass fraction to divide the spacecraft's dry mass into m_{MPE} and m_{cargo}. Note that rather than absolute dates and times, a combination of one absolute date and three relative durations are used, to aid convergence of the genetic algorithm [22] and remove the need for linear constraints to ensure that the dates are chronological.

Depending on the scenario, certain decision variables are superfluous, i.e.:

- Δt^O, Δt_{stay}, and λ_{MPE} are not needed for the scenarios including Earth as the source of material, since those scenarios do not include a mining phase.
- Δt^O and/or Δt^I are not needed for the transfers covered by Hohmann manoeuvres, only for those that include Lambert arcs.
- If *all* transfers are covered by Hohmann transfers, t^I_{dep} is not necessary.

Bounds are enforced on the decision variables in Eq.(12):

- 30 days $< \Delta t^O <$ 3 years
- 14 days $< \Delta t_{stay} <$ 3 years, to ensure that $t_{mining} > 0$, per Eq. (7)
- 30 days $< \Delta t^I <$ 3 years
- January 1st, 2025 $< t^I_{dep} <$ December 31st, 2050, to cover all synodic periods (time frame arbitrarily chosen)
- $0 < \lambda_{MPE} < 1$

These bounds are wide enough to accommodate all scenarios, thereby eliminating the need for individual fine-tuning of the genetic algorithm for each scenario. The genetic algorithm is initialized by 25 different seeds to increase the chances of finding the global optimum. It should be noted that most seeds result in very similar results, thus showing that the solutions are reliable.

The problem is also subject to a number of non-linear constraints. Non-linear constraints are included to enforce the minimum structural coefficient (ϵ_{min}) during all phases of the mission and that there is *at least* enough propellant to get to the destination. In case of an atmospheric entry, a mass penalty is applied to the structural mass through an additional structural coefficient, $\Delta\epsilon_{entry}$. Reference [44] states that the structural coefficient for SpaceX's Starship and DLR's SpaceLiner 7, both designed to be capable of multiple atmospheric entries, are 9.9% and 15.6%, respectively. The higher estimate for the structural coefficient of the SpaceLiner is linked to the intentionally robust design philosophy of the concept [44]. Therefore, it is assumed that $\epsilon_{entry} = 0.05$ is reasonable. For each transfer, it is checked whether $\frac{m_{dry}}{m_{wet}} \geq \epsilon$, where $\epsilon = \epsilon_{min}$ or $\epsilon = \epsilon_{min} + \Delta\epsilon_{entry}$, depending on whether (re)-entry is part of the scenario.

3. Results

This section presents the results obtained using the methodology in Section 2, for all material sources and customer locations as listed at the start of that section. Table 4 shows these results. For each scenario (i.e. combination of material source and customer location) for which the optimization algorithm found a solution, the specific cost (c in \$/kg), total mission duration (t_{mis} in years), required velocity change from material source to customer location (ΔV^I in km/s) and delivered mass ($m_{r,sold}$ in kg) are presented. For each scenario for which the optimization found no solution, meaning that the non-linear constraints could not be satisfied, no information is given. For scenarios involving Earth-based resources (first column), ΔV^I is the ΔV from the parking orbit (at 185 km [45]) to the destination, because there is only a cargo spacecraft directly from LEO, without a mining phase, as discussed in Section 2.1.

Note that the results in Table 4 are optimized individually for each departure/target pair and cannot be directly combined to create new scenarios. For example, results for the "NEA → Lunar surface" scenario and "Lunar surface → Lunar Gateway" scenario cannot be combined for a "NEA → Lunar surface → Lunar Gateway" mission. Each

Table 4: Results for all combinations of resource and customer locations. Legend in bottom-right corner. Specific-cost cells with the lowest value for each customer have been marked green.

Customer	Earth surface		Lunar surface		NEA (2000 SG344)		Martian surface		MBA (2015 AE282)	
Earth surface	**1**	0		0.39		1.63		-		-
		0	580	2.58	335	0.88	-	-	-	-
		∞		90.8		258.3		-		-
LEO (400 km)	**231**	∼0		0.47		1.46		-		5.01
		0.01	967	5.81	411	3.33	-	-	3,603	7.38
		118.6		55.0		204.4		-		20.6
GEO		∼0		0.47		1.46		-		5.04
	658	3.94	485	3.70	**250**	1.54	-	-	2,750	6.79
		41.7		109.6		336.6		-		27.1
SE-L_1		0.18		0.68		2.28		-		3.69
	661	3.81	427	3.18	**212**	0.55	-	-	9,655	8.93
		43.4		127.9		388.2		-		6.6
SE-L_2		0.18		0.66		1.49		-		3.69
	661	3.81	427	3.18	**214**	1.00	-	-	4,090	7.79
		43.4		127.7		397.6		-		15.7
Lunar surface		0.02		0.45		1.48		-		5.11
	1,279	5.92	**177**[1]	0	362	2.88	-	-	6,326	8.33
		21.5		299.9		232.8		-		11.8
Low lunar orbit		0.02		0.45		1.48		3.22		3.77
	665	3.96	291	1.91	**213**	0.92	19,387	7.74	2,289	6.42
		41.4		182.2		396.4		4.3		27.5
Lunar Gateway		0.01		0.49		1.48		-		3.76
	666	3.97	352	2.58	**216**	0.98	-	-	3,684	7.58
		41.3		151.3		389.1		-		17.6
Martian surface		0.90		1.46		1.75		1.09		4.07
	4,778	6.77	3,919	6.67	3,631	6.75	**336**[1]	0	1,987	4.42
		8.54		15.3		23.2		148.9		34.1
Mars Base Camp		0.56		1.36		1.72		1.03		2.95
	915	4.57	673	4.41	538	4.13	1,916	5.28	**511**	2.14
		34.2		88.3		155.6		25.9		114.2
SM-L_1		0.56		1.36		3.33		1.36		4.04
	1,563	6.11	1,104	5.87	1,085	5.91	2,455	5.70	**937**	3.92
		20.0		53.8		86.9		21.2		72.0
16 Psyche		-		-		-		-		4.45
	-	-	-	-	-	-	-	-	**916**	3.77
		-		-		-		-		76.8

[1] Specific cost based on one full cargo spacecraft, mining equipment can potentially last longer.

Legend:	c	[$/kg]
	t_{mis}	[years]
	ΔV^I	[km/s]
	$m_{r,sold}$	[tonnes]

scenario in Table 4 has been optimized for minimum specific cost. As part of this optimization, the spacecraft is sized according to the methodology in Section 2.3, resulting in a range of different-sized cargo spacecraft. In addition, the cargo spacecraft will not be completely filled with propellant at the start of the next transfer.

A more detailed overview of one example mission scenario, "NEA → Lunar Gateway", is given in Table 5. Table 5 shows that approximately 500 tonnes of propellant are produced, which is consistent with Ref. [23] and Ref. [31] when considering that the current paper includes electrolysis whereas Ref. [31] does not. Note that the launch date is in an arbitrarily-chosen time frame, as noted in Section 2.5, and this mission could be moved by a (number of) synodic period(s).

To emphasize that the goal of this work is to compare different scenarios, rather than give absolute values, Table 6 presents the *relative* metrics for the Lunar Gateway and Mars Base Camp. The specific cost for and delivered mass are normalized by the values for the scenarios involving a direct launch from the Earth's surface.

3.1. Discussion

There are a number of observations that stand out from Table 4. First, by far the lowest specific cost for $LOX/LH_2$for customers on the Earth, Lunar and Martian surface is realized by material sourced in the same location, rather than mining and processing elsewhere. Mining elsewhere and subsequent transport to surface locations means that a fraction of the propellant is used for this transfer, resulting in lower $m_{r,sold}$ than for the scenario where mining occurs on the same surface.

Furthermore, scenarios involving NEA 2000 SG344 show that this asteroid is in a strategic location, able to provide LOX/LH_2 to many destinations in the vicinity of Earth at the most competitive specific cost. Exceptions are customers at surface locations, as discussed before, and LEO, which is very close to the parking orbit after launch from the Earth surface. The reason for this is the relatively low ΔV^O from Earth escape to the NEA, which allows for a large part of the payload capacity of the launch vehicle to be used for structural mass, which in turn allows for a relatively large quantity of propellant to be transported. The ΔV^O to other sources are higher because the spacecraft either has to soft land on the Moon (for which $\Delta V = 1.963$ km/s, per Table 3), or transfer far from Earth to either Mars or the MBA, with a semi-major axis of 1.52 and 2.01 AU, respectively.

For customers further afield, in the vicinity of Mars and at the metallic main-belt asteroid 16 Psyche, MBA 2015 AE282 is able to provide resources at the lowest specific cost. Resources from this MBA could possibly even be used to support deep space missions outward from the main belt. However, Table 4 also shows that it is in general cost-prohibitive or infeasible to transport resources from the MBA back to customers in vicinity of the Earth, even if the target asteroid is positioned in the inner main belt, as is the case in Table 4. Besides the high specific cost, long mission durations are associated with scenarios selling to customers in the vicinity of the Earth. Long mission durations are unattractive for investors [46].

Another observation is related to scenarios mining and processing on the Martian surface. Table 4 shows that many scenarios are infeasible. This is due to two reasons. First, there is a mass penalty on the structural mass of the spacecraft because it has to withstand atmospheric entry (as discussed in Section 2.5) and second, there is a large ΔV cost for ascent from the Martian surface (4.026 km/s [41]). Because of the increase in minimum structural coefficient, the maximum ΔV decreases: $\Delta V_{max} = I_{sp} g_0 \log\left(1/(\epsilon_{min} + \Delta\epsilon_{entry})\right)$. Combined with the high ΔV for ascent, this means that many scenarios are not possible. Interestingly, scenarios mining and processing on the MBA perform better than those mining and processing on Mars, meaning that the larger semi-major axis of the MBA is outweighed by these two drawbacks for Mars. This is especially striking for customers at the Mars Base Camp: the specific cost is lower from all considered material sources other than the Martian surface.

In addition, high-thrust missions to Psyche are shown to be only possible by refuelling at an intermediate MBA, for the mission architecture defined here: a single stage from the LEO parking orbit to the destination using a hyperbolic trajectory to escape from the Earth. Of course other mission scenarios can be envisaged, but if a fully reusable launch vehicle such as SpaceX's Starship system is to be used, a parking orbit is unavoidable. On Psyche, water would be needed to mine metals on the metal-rich asteroid [27].

Finally, observations can be made regarding the total amount of volatiles delivered to the customer. Because the missions delivering Earth-

Table 5: Details for example mission "NEA → Lunar Gateway".

Parameter	**Value**
Launch date, t^O_{dep}	March 30$^{\text{th}}$, 2027
Transfer time outbound, Δt^O	213 days
ΔV^O	3.73 km/s
Stay time at NEA, Δt_{stay}	183 days
Mass cargo spacecraft, m_{cargo}	55.7 tonnes
Mining and processing equipment, m_{mpe}	2.31 tonnes
Produced LOX/LH_2, m_r	501 tonnes
Transfer time inbound, Δt^I	132 days
ΔV^I	0.982 km/s
Arrival date at customer	September 7$^{\text{th}}$, 2028
Mass delivered to Lunar Gateway, $m_{r,sold}$	389 tonnes

Table 6: Relative metrics for scenarios involving the Lunar Gateway or Mars Base Camp.

Material source location	**Lunar Gateway**		**Mars Base Camp**	
	c, normalized	**$m_{r,sold}$, normalized**	**c, normalized**	**$m_{r,sold}$, normalized**
Earth surface	1.000	1.000	1.000	1.000
Lunar surface	0.529	3.663	0.735	2.577
NEA (2000 SG344)	0.325	9.419	0.598	4.930
Martian surface	-	-	2.095	0.756
MBA (2015 AE282)	5.538	0.427	0.558	3.339

sourced volatiles are limited to the payload capacity of the launch vehicle, it is shown in Table 4 that $m_{r,sold}$ is relatively low to customers beyond GEO, compared to other sources. In contrast, scenarios mining and processing at NEA 2000 SG344 can deliver the largest quantity of volatiles to many destinations. This is because ΔV^O is low, as discussed above, and therefore a significant fraction of the payload capacity of the launch vehicle is dedicated to the structural mass of a large cargo spacecraft. In addition, ΔV^I is also relatively low for the NEA-scenarios, meaning that less propellant is "wasted" on the transfer to the customer.

In 2016, the United Launch Alliance set prices it is willing to pay for propellant in space in several locations. In a mid-term time frame, these prices are ∼$1,000 per kg at the Earth-Moon L_1-point and ∼$500 per kg on the Lunar surface [47]. Comparing these costs with Table 4, and assuming that propellant will not be sold at cost price but will include a mark-up, it is clear that delivery of propellant from the Earth will not meet these prices in the vicinity of the Moon, but mining on the Lunar surface or a NEA will be required. Whilst this study focuses on delivery to customers located at the final location in space, the commercial enterprise mining and processing these space-based resources can also choose to use these resources themselves, which would remove the need for a mark-up on the price.

It is worth noting that $m_{r,sold}$ does not have to consist of the combination of LOX and LH_2 suitable for rocket propellant per se, but $m_{r,sold}$ could consist of any other water-derived resource [48]. For example, instead of venting and therefore discarding oxygen, it can also be transported, such that customers only have to bring the (much lighter) LH_2 and can buy the (heavy) LOX in space. This way, less mined resources are wasted through venting and therefore the specific cost can be brought down. Also, pure water could be transported, which would also allow for a reduction in cost because less oxygen has to be vented and less water has to be electrolyzed. For any resource other than the combination of LOX/LH_2 used, the analysis would have to be carried out with slightly varied input values for the throughput rate, r, and/or the mixture ratio, λ_{MR}. When transporting different resources than LOX/LH_2, care should be taken that there is sufficient propellant left in the spacecraft to transfer to the final destination, in the case that no in-situ

propellant can be used.

It can be noted however, that the costs presented in this paper will have significant uncertainty and risks are likely weighted strongly towards the increased costs. Dependency on intermediate missions advancing technology readiness and planning for the mid- to far-term time frame adds to the inherent uncertainties of cost estimation. Nonetheless, the results presented here can be used to focus future research on potentially more profitable and feasible missions. More importantly, the relative metrics, such as those shown in Table 6 can be used to shape future research and mission design. Table 6 confirms the preferred selection of the material source for customers at the Lunar Gateway and Mars Base Camp, without relying on the absolute specific costs presented in Table 4, which have a higher uncertainty.

4. Sensitivity analysis

This section presents a sensitivity analysis for a number of input parameters to the model. Because of the assumptions in the cost model and the inherent uncertainty of planning future missions, a sensitivity analysis is important. First, a range of Monte Carlo analyses investigates the sensitivity of the model to relevant input parameters. Next, the effect of some assumptions in the cost model are investigated. Also, the impact of asteroid selection (both near-Earth and main-belt) is examined. Rather than producing a series of tables like Table 4, these sensitivity analyses are carried out for a smaller number of relevant scenarios, which depend on the input parameter under investigation.

4.1. Monte Carlo analysis

Due to the highly non-linear nature of the optimizations in this paper, a Monte Carlo simulation is considered appropriate to assess the uncertainty of the results based on uncertainty of the input parameters. For the Monte Carlo analysis, the following input parameters are regarded as relevant: specific impulse (I_{sp}), minimum allowed structural coefficient (ϵ_{min}) and the additional structural coefficient for atmospheric entry (ϵ_{entry}), cost elements for development, manufacturing, launch and operations (C_{dev}, C_{man}, C_l, C_{op}), throughput rate (r) and launch vehicle payload capacity (m_l). For these input variables, the scenarios "NEA $\rightarrow$ Lunar Gateway" and "NEA $\rightarrow$ Mars Base Camp" are investigated. These two are considered due to their potential for human exploration and the corresponding need for propellant and other water-based resources, as well as their affordability in Table 4. In addition, for the uncertainty in r, "Lunar Surface $\rightarrow$ Lunar Gateway" and "Mars $\rightarrow$ Mars Base Camp" are considered, to investigate the sensitivity to r on other material source locations besides NEAs. For ϵ_{entry}, "Mars $\rightarrow$ Mars Base Camp" is considered instead of "NEA $\rightarrow$ Lunar Gateway" and "NEA $\rightarrow$ Mars Base Camp", because ϵ_{entry} is not applicable in those scenarios.

The uncertainty on the input parameters is modelled using a Gaussian probability density function, with the mean value as described in Section 2, and a standard deviation is chosen as 10% of this value. This standard deviation is arbitrarily chosen and does not necessarily reflect the actual uncertainty, but this does provide a means to assess the sensitivity of each parameter with respect to the others. The Monte Carlo simulations are performed for each input parameter separately by optimizing the scenario using one changed input. For each considered scenario for each input parameter, a total of 500 pseudo-random samples of the input parameter are used to initialize the optimization. The specific cost is subsequently optimized for each instance, following the procedure described in Section 2. The resulting distributions of specific costs are visualized using boxplots in Figs. 4-7. For each boxplot, the central line indicates the median value and the box contains 50% of the results, with the bottom and top edges of the box marking the 25^{th} and 75^{th} percentiles, respectively. The dashed lines extend to the most extreme results not considered outliers, with the outliers are plotted individually in red. Due to how the uncertainties on the input parameters are modelled, the boxplots present clear indications of how sensitive the solution is to an equal relative change in the input parameters. The Monte Carlo simulations have been distributed over Figs. 4-7 in a way that allows for meaningful comparison with other simulations. Note that within Fig. 6 and 7 the vertical axis spans an equal range, but centered around a different specific cost, to allow for comparison.

From Figs. 4 and 5 it is apparent that the minimum specific cost is most sensitive to uncertainties in the imposed minimum structural coefficient for the spacecraft and the manufacturing cost. Also, uncertainties in the development cost have a relatively small effect on the specific cost of the mined

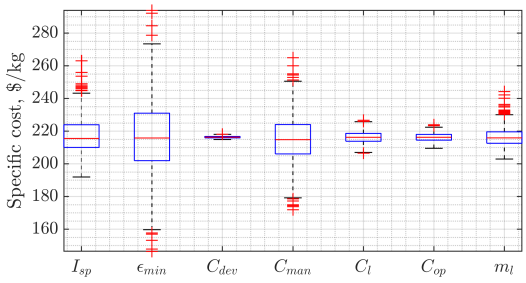

Figure 4: Resulting boxplots of Monte Carlo simulations for I_{sp}, ϵ_{min}, C_{dev}, C_{man}, C_l, C_{op} and m_l, for scenario NEA → Lunar Gateway.

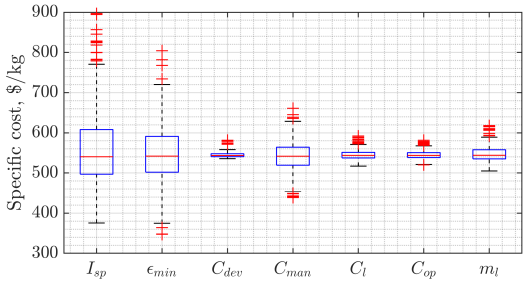

Figure 5: Resulting boxplots of Monte Carlo simulations for I_{sp}, ϵ_{min}, C_{dev}, C_{man}, C_l, C_{op} and m_l, for scenario NEA → Mars Base Camp.

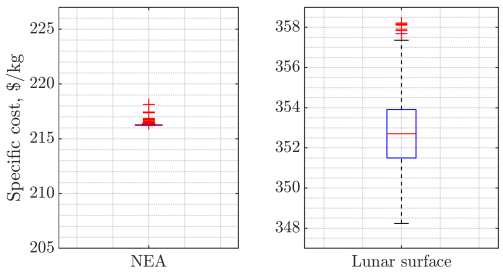

Figure 6: Resulting boxplots of Monte Carlo simulations for r, for scenarios to Lunar Gateway.

resources. The observations are the same for both the Lunar Gateway and Mars Base Camp scenarios. From Figs. 6 and 7 it is evident that the throughput rate also has a relatively minor effect, especially when comparing the vertical axis range with Figs. 4 and 5. It is shown that the sensitivity to the throughput rate differs slightly depending on the mining location, but the sensitivity is still minimal. In addition to this Monte Carlo simulation, which assumes a 10% standard deviation for the throughput rate, Table 7 shows the impact of

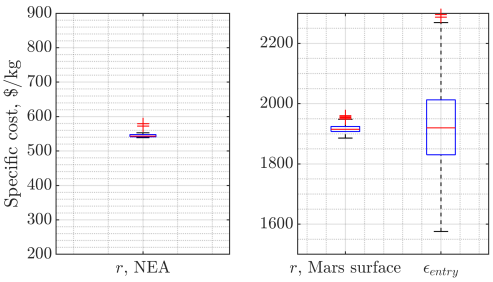

Figure 7: Resulting boxplots of Monte Carlo simulations for r, for scenarios to Mars Base Camp, and Monte Carlo simulation for ϵ_{entry}.

smaller throughput rates for the "NEA → Lunar Gateway" and "NEA → Mars Base Camp" scenarios, beyond the 10% standard deviation. While Table 7 shows that the specific cost to produce LOX/LH_2 increases, as expected, it also shows that the impact is rather limited, even for dramatically lower throughput rates. Other simulated scenarios, not presented in Table 7, show very similar trends: that to offset the decrease in throughput rate, the stay time at the source is increased, which has an impact on the operational costs as per Eq. (1).

Table 7: Effect on specific cost (in $/kg) of lower throughput rates, for the baseline mission from a NEA.

Multiplier	**Lunar Gateway**	**Mars Base Camp**
1×	216	538
1/2×	224	562
1/5×	245	594
1/10×	262	624
1/20×	296	689

Where Figs. 4 and 5 show a relatively large sensitivity to the minimum structural coefficient, Fig. 7 shows that the specific cost is also relatively sensitive to the imposed additional structural coefficient for atmospheric entry. Because the spacecraft on which ϵ_{entry} is based have not yet flown, and could experience mass growth, this sensitivity is especially important. Future research should take this sensitivity into account. These observations are consistent with those in Ref. [23].

4.2. Cost model assumptions

The methodology described in Section 2 and Refs. [22, 23] assumes aviation-like costs for development and manufacturing costs elements. It is assumed that technology has matured sufficiently

through intermediate missions, because of the mid- to far-term time frame considered for the missions described in this paper. Since there is significant uncertainty on when this time frame will occur, a sensitivity analysis has been carried out with higher development and manufacturing costs. To achieve this, the production volume has been varied, which, as described in Ref. [22], directly influences the development and manufacturing costs. The total development cost is spread evenly over all units in the production volume, while the manufacturing cost experiences the learning curve effect [49].

Table 8 shows the effect of changing the production volume for two scenarios: "NEA → Lunar Gateway" and "NEA → Mars Base Camp". In the methodology of this paper and Refs. [22, 23], a production volume of 2,033 units is used, based on the production volume of the Boeing 777[1]. This sensitivity analysis investigates the effect of using from 1 to 10,000 units in various steps, by optimizing the missions again with the different development and manufacturing costs resulting from the production volume. Table 8 shows that, for the two investigated scenarios, in order to have specific costs under $1,000, the production volume has to be at least 100 units, when assuming the cost model adopted in this paper. Note that these units do not necessarily have to be for the exact same mission, but that development/manufacturing costs can also be brought down when other large deep-space cargo spacecraft are designed and built. In more general terms, the specific costs for the two investigated scenarios are under $1,000 when development costs are able to reach the level of ∼$750 per kg and manufacturing cost of ∼$1,500 per kg, regardless of the cost model used.

The next sensitivity analysis is aimed at the development and manufacturing cost for the MPE. While industry has significant experience designing and building spacecraft, this is not necessarily the case for designing and building MPE. To this extent, the impact of higher development/manufacturing costs for MPE is investigated. Table 9 shows the resulting specific cost for two scenarios: "NEA → Lunar Gateway" and "NEA → Mars Base Camp", considering that development/manufacturing cost for MPE are n times the baseline, which is still used for the spacecraft in the re-optimized scenarios. As shown in Table 9, even when the development and manufacturing costs for MPE are 10 times as high, the specific cost per delivered kg of propellant to the Lunar Gateway and Mars Base Camp only changes by 18 and 15%, respectively.

4.3. Different asteroids

To investigate the influence of the target selection for the asteroids, both near-Earth and main-belt asteroids, a sensitivity analysis is carried out. At the time of writing, there are 23,390 NEAs and 938,938 MBAs catalogued in the Horizons database[2].

The NEA targeted in the baseline scenario, 2000 SG344, has Earth-like orbital elements: semi major axis $a = 1.116$ AU, eccentricity $e = 0.151$ and inclination $i = 0.943°$. This allows for low ΔVs to and from the Earth, but not necessarily to Mars, for example. To this extent, the algorithm is executed using all discovered NEAs [35], to assess the effect of asteroid selection. The asteroids with the lowest specific cost to the Martian surface, Mars Base Camp, SM-L_1 and Psyche are given in Table 10. Upon comparison with Table 4, it is clear that asteroid selection is very important for the separate destinations. Specific costs for customers at the Martian surface, Mars Base Camp, and SM-L_1 are all much lower if an asteroid is selected which is appropriate for this scenario, with orbital elements similar to those of Mars. This ensures a low ΔV^I which in turn ensures that only a small fraction of mined resources is used for transportation to the customer. Where Table 4 shows that for NEA 2000 SG344, Psyche is out of reach, Table 10 shows that appropriate asteroid selection for this customer allows for a specific cost as low as $951 per kg using the adopted cost model. The selected asteroid has perihelion close to Earth (1.26 AU) and aphelion close to Psyche's orbit (2.835 AU for the NEA and a semi-major axis of 2.921 AU for Psyche), again aiming to especially minimize ΔV^I to reduce the consumption of propellant for transportation.

Similarly, the MBA targeted in the baseline scenario is positioned in the *inner* main belt, at $a = 2.015$ AU, $e = 0.173$ and $i = 0.477°$. The inner main belt stretches between $2.0 < a < 2.5$ AU and the middle main belt between $2.5 < a < 2.82$ AU. This asteroid was selected due to its relative proximity to the Earth. However, again, this does not necessarily imply that it is the optimal asteroid for

[1] `http://www.boeing.com/commercial/#/orders-deliveries`, accessed May 31st, 2019

[2] Obtained on August 20th, 2020 [35]

Table 8: Effect on specific cost (in $/kg) of changing the production volumes for the baseline mission from a NEA.

Production volume	C_{dev}	C_{man}	Lunar Gateway	Mars Base Camp
1	75,600	2,875	10,917	27,663
10	7,560	2,094	1,456	3,590
100	756	1,525	400	987
500	151	1,222	265	664
1,000	76	1,111	238	593
2,033	38	1,010	**216**	**538**
5,000	15	890	195	490
10,000	7	809	182	458

Table 9: Effect on specific cost (in $/kg) of higher specific development and manufacturing cost for MPE, for the baseline mission from a NEA.

Multiplier	Lunar Gateway	Mars Base Camp
1×	216	538
1.25×	218	545
1.50×	219	550
2×	222	554
2.50×	225	561
3×	228	565
4×	233	575
5×	238	601
10×	257	620

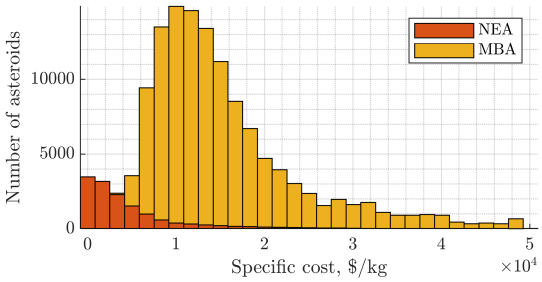

Figure 8: Histogram of available asteroids for scenarios to Lunar Gateway.

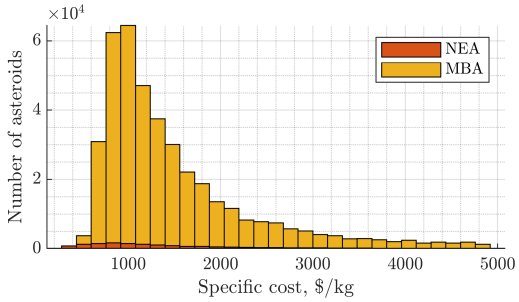

Figure 9: Histogram of available asteroids for scenarios to Mars Base Camp.

destinations further afield. Due to the sheer number of MBAs, 938,938[2] at the time of writing, it is computationally unrealistic to run the algorithm on all MBAs. Instead, 20,000 MBAs are selected at random and results are extrapolated to the entire set. Because of this approach, a table similar to Table 10 cannot be produced. However, other meaningful conclusions can still be drawn. Table 11 shows the quantity of NEAs and MBAs available for mining for customers at the various locations, for a range of minimum specific costs. In addition, Figures 8 and 9 show the distribution of these specific costs as histograms for the Lunar Gateway and Mars Base Camp, respectively.

Table 11 shows that for most customers, transferring to the main-belt and back is not beneficial, compared to transferring to an NEA. This is especially evident in the column $c < 2,000$ $/kg, where it can be seen that there are no MBAs available to deliver propellant under $2,000 per kg to customers in the vicinity of the Earth, including the nearby collinear Lagrange points and customers on or near the Moon. For customers on or near Mars and Psyche, there is a a wider range of asteroids to choose from for affordable propellant. Even though there are many MBAs to select with $c < 1,000$ $/kg, for the Mars-customers (on the surface, in the Mars Base Camp and in SM-L1) it is still cheaper to select an NEA. Only once these NEAs have been depleted, is it more efficient to use MBAs.

Figures 8 and 9 show more detail for the scenarios to the Lunar Gateway and Mars Base Camp, to illustrate the trends visible in Table 11 for customers near the Earth/Moon and customers near Mars, respectively. Note that the histograms are stacked to reflect the total number of available as-

Table 10: NEAs with lowest specific cost for destinations at Mars and beyond.

Customer location	**Minimum specific cost [$/kg]**	**Asteroid designation**	**Semi-major axis [AU]**	**Eccentricity**	**Inclination [deg]**
Martian surface	592	2005 UK5	1.420	0.087	2.609
Mars Base Camp	260	2017 QN17	1.391	0.095	2.540
SM-L1	295	2001 FC7	1.436	0.115	2.621
16 Psyche	951	2017 HK49	2.011	0.384	2.138

Table 11: Number of available asteroids for a certain specific cost, c [$/kg].

Customer	**c < 250**		**c < 500**		**c < 1,000**		**c < 2,000**		**c < 5,000**	
location	**NEA**	**MBA**	**NEA**	**MBA**	**NEA**	**MBA**	**NEA**	**MBA**	**NEA**	**MBA**
Earth surface	0	0	28	0	341	0	1.3k	0	3.1k	0
LEO (400 km)	0	0	13	0	1.4k	0	5.2k	0	11.7k	2.3k
GEO	0	0	371	0	2.3k	0	5.7k	0	11.7k	113k
SE-L1	1	0	173	0	1.1k	0	2.7k	0	5.5k	0
SE-L2	4	0	262	0	1.5k	0	3.7k	0	7.8k	0
Lunar surface	0	0	35	0	868	0	2.8k	0	6.5k	0
Low lunar orbit	3	0	696	0	2.9k	0	6.5k	0	12.3k	33.1k
Lunar Gateway	2	0	346	0	1.8k	0	4.2k	0	8.9k	0
Martian surface	0	0	0	0	55	0	799	47	3.4k	12.4k
Mars Base Camp	0	0	757	0	5.3k	92.6k	11.5k	310k	15.3k	391k
SM-L1	0	0	72	0	1.2k	188	4.3k	114k	10.0k	300k
16 Psyche	0	0	0	0	8	100k	2.0k	318k	7.8k	378k

teroids and that the scale on the horizontal and vertical axes are not the same for the two figures. In order to show meaningful results, the range for specific costs is 10 times higher for the Lunar Gateway compared to the Mars Base Camp, indicating that the specific cost is much higher for many available asteroids. Also, the horizontal axis, the number of asteroids per bin, is three times as high for the Mars Base Camp, revealing that there are more asteroids available for customers there. These figures highlight that mining on NEAs in general results in cheaper resources, but that there are many more MBAs available. This conclusion can be drawn regardless the uncertainty on inputs for the cost model. This has implications for long-term SRU where extraction of asteroid resources changes the large-scale distribution of resources in the inner solar system.

5. Conclusion

In this paper, an investigation into the economic and commercial potential of space resource utilization (SRU) on the surface of the Moon, Mars, a near-Earth asteroid and a main-belt asteroid is presented. Results are compared with lifting the same resources from the Earth's surface. Economic modelling and trajectory optimization are coupled in a bid to find the minimum specific cost to deliver propellant, more specifically LOX/LH_2, from these bodies to a number of customer locations. Various customer locations are considered: on the surface, in orbit around, or at a Lagrange point near the Earth, Moon, and Mars, as well as on Psyche, a large metallic main-belt asteroid. A generic mission scenario is established and, where necessary, refined for specific combinations of resource and customer locations. This generic mission scenario, as well as the unified approach to optimization, allows for a fair comparison of the different mission scenarios to specific resource and customer locations. This mission scenario includes launch using a reusable launch vehicle transporting a cargo spacecraft equipped with mining and processing equipment, and hyperbolic transfers to and from the re-

source location.

Results show that, for customers on the Earth, Moon and Mars, the minimum specific cost is found when mining and processing of water in LOX/LH_2 occurs on the same surface. For any customer beyond LEO, SRU is cheaper than directly launching the resources from the Earth and the total mass delivered using one launch/cargo spacecraft can be leveraged several times. The near-Earth asteroid considered, 2000 SG344, is in a very strategic location for most customers in the vicinity of the Earth, except those on the surface of the Earth and Moon and in LEO, as noted earlier. The reason for this is a relatively low outbound ΔV from Earth escape to the asteroid. The outbound ΔV for other sources are higher because the spacecraft either has to soft land on the Moon, or transfer far from Earth to either Mars or the selected (inner) main-belt asteroid, with a semi-major axis of 1.52 and 2.01 AU, respectively. For customers further away, i.e. near Mars and on Psyche, mining and processing on a main-belt asteroid is most cost effective, at least among the considered baseline material sources. Furthermore, results show that it is generally infeasible to mine and process on the Martian surface and transport these resources to a customer in the vicinity of the Earth. This is due to an imposed mass penalty, to cope with atmospheric entry on Mars and the high ΔV for ascent from the Martian surface.

Several types of sensitivity analyses have been performed. First, a range of Monte Carlo simulations on key input parameters show that the resulting specific cost is relatively most sensitive to the manufacturing costs of the spacecraft and the imposed minimum structural coefficient, and least sensitive to uncertainties on the development costs and throughput rate. Second, it is shown that in order for specific costs to be in an acceptable range, development and manufacturing costs have to be lower than ∼\$750 and ∼\$1,500 per kg, respectively, regardless of the cost model used. Last, the impact of asteroid selection is examined, where results show that for all customers considered, except Psyche, there are near-Earth asteroids which are cheaper than the cheapest main-belt asteroid. Only in the long term when these near-Earth asteroids have been depleted, is it financially worth transferring to a main-belt asteroid and back. This range of sensitivity analyses show that the relative metrics for the different scenarios remain similar when exposed to the same change of an input parameter, meaning that conclusions are valid even when faced with the inevitable uncertainties regarding future mission planning.

Concluding, for customers beyond LEO, SRU can and should be used rather than lifting water-derived resources from the Earth's surface. Despite significant uncertainties on input parameters for the model, the modelling efforts in this paper may help inform the selection of SRU sources for specific mission scenarios, ultimately resulting in lower cost, mass and risk for future human and robotic space exploration.

6. Acknowledgements

Merel Vergaaij gratefully acknowledges the College of Science and Engineering at the University of Glasgow for supporting this work.

Colin McInnes was supported by a Royal Society Wolfson Research Merit Award and a Royal Academy of Engineering Chair in Emerging Technologies.

References

[1] G. Sanders, W. Larson, K. Sacksteder, C. Mclemore, NASA In-Situ Resource Utilization (ISRU) Project: Development and Implementation, in: AIAA SPACE 2008 Conference & Exposition, American Institute of Aeronautics and Astronautics, San Diego, California, 2008. doi:10.2514/6.2008-7853.
URL http://arc.aiaa.org/doi/10.2514/6.2008-7853

[2] K. Hadler, D. Martin, J. Carpenter, J. Cilliers, A. Morse, S. Starr, J. Rasera, K. Seweryn, P. Reiss, A. Meurisse, A universal framework for Space Resource Utilisation (SRU), Planetary and Space Science 182 (2020) 104811. doi:10.1016/j.pss.2019.104811.
URL https://linkinghub.elsevier.com/retrieve/pii/S0032063319301849

[3] G. Sanders, In Situ Resource Utilization on Mars - Update from DRA 5.0 Study, in: 48th AIAA Aerospace Sciences Meeting Including the New Horizons Forum and Aerospace Exposition, American Institute of Aeronautics and Astronautics, Orlando, Florida, 2010. doi:10.2514/6.2010-799.
URL http://arc.aiaa.org/doi/10.2514/6.2010-799

[4] T. Sarton du Jonchay, H. Chen, A. Wieger, Z. Szajnfarber, K. Ho, Space architecture design for commercial suitability: A case study in in-situ resource utilization systems, Acta Astronautica (2020) S0094576520302952doi:10.1016/j.actaastro.2020.05.012.

[5] D. G. Andrews, K. D. Bonner, A. W. Butterworth, H. R. Calvert, B. R. H. Dagang, K. J. Dimond, L. G. Eckenroth, J. M. Erickson, B. A. Gilbertson, N. R. Gompertz, O. J. Igbinosun, T. J. Ip, B. H. Khan, S. L. Marquez, N. M. Neilson, C. O. Parker, E. H. Ransom, B. W. Reeve, T. L. Robinson, M. Rogers, P. M. Schuh, C. J. Tom, S. E. Wall, N. Watanabe, C. J.

Yoo, Defining a successful commercial asteroid mining program, Acta Astronautica 108 (2015) 106–118. doi:10.1016/j.actaastro.2014.10.034.

[6] M. B. Duke, B. R. Blair, J. Diaz, Lunar resource utilization: Implications for commerce and exploration, Advances in Space Research 31 (11) (2003) 2413–2419. doi:10.1016/S0273-1177(03)00550-7.
URL https://linkinghub.elsevier.com/retrieve/pii/S0273117703005507

[7] R. Mitchell, Into the Final Frontier: The Expanse of Space Commercialization, Missouri Law Review 83 (2) 429–454.

[8] D. Rapp, Use of Extraterrestrial Resources for Human Space Missions to Moon or Mars, 2018.

[9] R. Mueller, P. Van Susante, A Review of Lunar Regolith Excavation Robotic Device Prototypes, in: AIAA SPACE 2011 Conference & Exposition, American Institute of Aeronautics and Astronautics, Long Beach, California, 2011. doi:10.2514/6.2011-7234.
URL http://arc.aiaa.org/doi/10.2514/6.2011-7234

[10] V. Badescu (Ed.), Moon: Prospective Energy and Material Resources, Springer Berlin Heidelberg, Berlin, Heidelberg, 2012. doi:10.1007/978-3-642-27969-0.
URL http://link.springer.com/10.1007/978-3-642-27969-0

[11] K. Sacksteder, G. Sanders, In-Situ Resource Utilization for Lunar and Mars Exploration, in: 45th AIAA Aerospace Sciences Meeting and Exhibit, American Institute of Aeronautics and Astronautics, Reno, Nevada, 2007. doi:10.2514/6.2007-345.
URL http://arc.aiaa.org/doi/10.2514/6.2007-345

[12] M. Anand, I. Crawford, M. Balat-Pichelin, S. Abanades, W. van Westrenen, G. Péraudeau, R. Jaumann, W. Seboldt, A brief review of chemical and mineralogical resources on the Moon and likely initial in situ resource utilization (ISRU) applications, Planetary and Space Science 74 (1) (2012) 42–48. doi:10.1016/j.pss.2012.08.012.
URL https://linkinghub.elsevier.com/retrieve/pii/S0032063312002498

[13] J. E. Kleinhenz, A. Paz, An ISRU propellant production system for a fully fueled Mars Ascent Vehicle, in: 10th Symposium on Space Resource Utilization, American Institute of Aeronautics and Astronautics, Grapevine, Texas, 2017. doi:10.2514/6.2017-0423.
URL http://arc.aiaa.org/doi/10.2514/6.2017-0423

[14] H. Benaroya, Architecture for an Asteroid-Mining Spacecraft, in: V. Badescu (Ed.), Asteroids, Springer Berlin Heidelberg, Berlin, Heidelberg, 2013, pp. 403–413. doi:10.1007/978-3-642-39244-3_16.
URL http://link.springer.com/10.1007/978-3-642-39244-3_16

[15] J. C. Sercel, C. E. Peterson, J. R. French, A. Longman, S. G. Love, R. Shishko, Stepping stones: Economic analysis of space transportation supplied from NEO resources, in: 2018 IEEE Aerospace Conference, IEEE, Big Sky, MT, 2018, pp. 1–21. doi:10.1109/AERO.2018.8396702.
URL https://ieeexplore.ieee.org/document/8396702/

[16] D. D. Mazanek, R. G. Merrill, J. R. Brophy, R. P. Mueller, Asteroid Redirect Mission concept: A bold approach for utilizing space resources, Acta Astronautica 117 (2015) 163–171. doi:10.1016/j.actaastro.2015.06.018.
URL https://linkinghub.elsevier.com/retrieve/pii/S0094576515002635

[17] R. Shishko, R. Fradet, S. Do, S. Saydam, C. Tapia-Cortez, A. G. Dempster, J. Coulton, Mars Colony in situ resource utilization: An integrated architecture and economics model, Acta Astronautica 138 (2017) 53–67. doi:10.1016/j.actaastro.2017.05.024.
URL https://linkinghub.elsevier.com/retrieve/pii/S0094576517305131

[18] C. A. Jones, J. Klovstad, E. Judd, D. Komar, Cost Breakeven Analysis of Cis-lunar ISRU for Propellant, in: AIAA Scitech 2019 Forum, American Institute of Aeronautics and Astronautics, San Diego, California, 2019. doi:10.2514/6.2019-1372.
URL https://arc.aiaa.org/doi/10.2514/6.2019-1372

[19] N. J. Bennett, D. Ellender, A. G. Dempster, Commercial viability of lunar In-Situ Resource Utilization (ISRU), Planetary and Space Science 182 (2020) 104842. doi:10.1016/j.pss.2020.104842.
URL https://linkinghub.elsevier.com/retrieve/pii/S0032063319301163

[20] M. J. Sonter, The technical and economic feasibility of mining the near-Earth asteroids, Acta Astronautica 41 (4-10) (1997) 637–647. doi:10.1016/S0094-5765(98)00087-3.

[21] O. Trivailo, M. Sippel, Y. A. Sekercioğlu, Review of hardware cost estimation methods, models and tools applied to early phases of space mission planning, Progress in Aerospace Sciences 53 (2012) 1–17. doi:10.1016/j.paerosci.2012.02.001.

[22] M. Vergaaij, C. R. McInnes, M. Ceriotti, Economic assessment of high-thrust and solar-sail propulsion for near-Earth asteroid mining, Advances in Space Research (2020) S0273117720304142doi:10.1016/j.asr.2020.06.012.
URL https://linkinghub.elsevier.com/retrieve/pii/S0273117720304142

[23] M. Vergaaij, C. McInnes, M. Ceriotti, Influence of Launcher Cost and Payload Capacity on Asteroid Mining Profitability, Journal of the British Interplanetary Society 72 (12) (2019) 435–444.

[24] T. Cichan, S. A. Bailey, S. D. Norris, R. P. Chambers, S. D. Jolly, J. W. Ehrlich, Mars Base Camp: An architecture for sending humans to Mars by 2028, in: 2017 IEEE Aerospace Conference, IEEE, Big Sky, MT, USA, 2017, pp. 1–18. doi:10.1109/AERO.2017.7943981.
URL http://ieeexplore.ieee.org/document/7943981/

[25] T. J. Colvin, K. Crane, B. Lal, Assessing the economics of asteroid-derived water for propellant, Acta Astronautica 176 (2020) 298–305. doi:10.1016/j.actaastro.2020.05.029.
URL https://linkinghub.elsevier.com/retrieve/pii/S009457652030312X

[26] T. D. Haws, J. S. Zimmerman, M. E. Fuller, SLS, the Gateway, and a Lunar Outpost in the Early 2030s, in: 2019 IEEE Aerospace Conference, IEEE, Big Sky, MT, USA, 2019, pp. 1–15. doi:10.1109/AERO.2019.8741598.
URL https://ieeexplore.ieee.org/document/8741598/

[27] V. Hessel, N. N. Tran, S. Orandi, M. R. Asrami, M. E. Goodsite, H. Nguyen, Continuous-Flow Extraction of Adjacent Metals - a Disruptive Economic Window for

In-Situ Resource Utilization of Asteroids?, Angewandte Chemie International Edition (Jan. 2020). doi:10.1002/anie.201912205.

[28] E. Musk, Making life multi-planetary, New Space 6 (1) (2018) 2–11. doi:10.1089/space.2018.29013.

[29] M. Sonter, The Technical and Economic Feasibility of Mining the Near-Earth Asteroids, Thesis Master of Science, Department of Physics and Department of Civil and Mining Engineering, University of Wollongong, Wollongong (1996).
URL https://ro.uow.edu.au/cgi/viewcontent.cgi?article=3862&context=theses

[30] M. Sonter, Near earth objects as resources for space industrialization, Solar System Development Journal 1 (1) (2001) 1–31.

[31] A. M. Hein, R. Matheson, D. Fries, A techno-economic analysis of asteroid mining, Acta Astronautica 168 (2020) 104–115. doi:10.1016/j.actaastro.2019.05.009.

[32] B. R. Blair, J. Diaz, M. B. Duke, E. Lamassoure, R. Easter, M. Oderman, M. Vaucher, Space Resource Economic Analysis Toolkit: The Case for Commercial Lunar Ice Mining, Final Report to the NASA Exploration Team (Dec. 2002).

[33] G. P. Sutton, O. Biblarz, Rocket Propulsion Elements, eighth Edition, John Wiley & Sons, 2010.

[34] Jet Propulsion Laboratory, Solar system dynamics: Ephemerides (2016).
URL http://ssd.jpl.nasa.gov/?ephemerides

[35] Jet Propulsion Laboratory, JPL Small-Body Database Search Engine (Aug. 2020).
URL https://ssd.jpl.nasa.gov/sbdb_query.cgi

[36] D. Izzo, Revisiting Lambert's problem, Celestial Mechanics and Dynamical Astronomy 121 (1) (2015) 1–15. doi:10.1007/s10569-014-9587-y.

[37] Wooster, Keynote talk: SpaceX's Plans for Sending Humans to Mars, in: 22nd Annual Mars Society Convention, University of Southern California, CA, USA, 2019.
URL youtu.be/9SZ3mVGBiiI

[38] SpaceX, Vehicle Landing (Oct. 2017).
URL https://www.youtube.com/watch?v=5seefpjMQJI

[39] B. G. Drake, K. D. Watts, Human Exploration of Mars Design Reference Architecture 5.0, Addendum #2, Tech. Rep. NASA/SP–2009-566-ADD2 (Mar. 2014).

[40] B. Donahue, G. Caplin, D. Smith, Lunar Lander Concept Design for the 2019 NASA Outpost Mission, in: AIAA SPACE 2007 Conference & Exposition, American Institute of Aeronautics and Astronautics, Long Beach, California, 2007. doi:10.2514/6.2007-6175.
URL http://arc.aiaa.org/doi/10.2514/6.2007-6175

[41] J. V. Bowles, L. C. Huynh, V. M. Hawke, X. J. Jiang, Mars Sample Return: Mars Ascent Vehicle Mission and Technology Requirements, Technical Report NASA/TM-2013-216620, ARC-E-DAA-TN12232, NASA Ames Research Center; Moffett Field, CA, United States (Nov. 2013).

[42] P. Cage, I. Kroo, R. Braun, Interplanetary trajectory optimization using a genetic algorithm, in: Astrodynamics Conference, American Institute of Aeronautics and Astronautics, 1994. doi:10.2514/6.1994-3773.

[43] M. Vasile, E. Minisci, M. Locatelli, Analysis of Some Global Optimization Algorithms for Space Trajectory Design, Journal of Spacecraft and Rockets 47 (2) (2010) 334–344. doi:10.2514/1.45742.
URL https://arc.aiaa.org/doi/10.2514/1.45742

[44] M. Sippel, S. Stappert, A. Koch, Assessment of multiple mission reusable launch vehicles, Journal of Space Safety Engineering 6 (3) (2019) 165–180. doi:10.1016/j.jsse.2019.09.001.
URL https://linkinghub.elsevier.com/retrieve/pii/S2468896719300886

[45] G. Gargioni, D. Alexandre, M. Peterson, K. Schroeder, Multiple Asteroid Retrieval Mission from Lunar Orbital Platform-Gateway Using Reusable Spacecrafts, in: 2019 IEEE Aerospace Conference, IEEE, 2019. doi:10.1109/aero.2019.8741985.

[46] R. Gertsch, L. Gertsch, Economic Analysis Tools for Mineral Projects in Space, Space Resources Roundtable (2005).

[47] L. David, Inside {ULA's} Plan to Have 1,000 People Working in Space by 2045, Space.com (Jun. 2016).
URL https://www.space.com/33297-satellite-refueling-business-proposal-ula.html

[48] S. Dorrington, J. Olsen, A location-routing problem for the design of an asteroid mining supply chain network, Acta Astronautica 157 (2019) 350–373. doi:10.1016/j.actaastro.2018.08.040.

[49] J. Markish, Valuation Techniques for Commercial Aircraft Program Design, PhD thesis, Massachusetts Institute of Technology (Jun. 2002).